ICANS-XI International Collaboration on Advanced Neutron Sources
KEK, Tsukuba, October 22-26, 1990

Neutron Production in Thick Lead Target by 1-3.7 GeV Protons and Deuterons

V. A. Nikolaev, V. I. Yurevich, R. M. Yakovlev
V. G. Khlopin Radium Institute, Leningrad 197022, USSR

R. G. Vassil'kov
Moscow Radiotechnical Institute, Moscow 113519, USSR

The neutron field of thick lead target (20 cm diam. and 60 cm long) has been studied using the method of threshold detectors - fission and spallation detectors with SSNTD's. The investigation has been carried out at proton and deuteron beams of synchrophasotron JINR in the energy range 1-3.7 GeV. The dependence of the differential neutron distributions on a type of incident projectile and on ion energy are discussed. The data analysis has shown, that the neutron spectra for incident protons are more hard than for the deuteron beam. The relative partial neutron yields for low-energy component (<1 MeV) and high-energy component (>20 MeV) contain 38%, 10% and 45%, 7% for p and d ions respectively . The average value of the total neutron yields ratio Y_d/Y_p = 1.20±0.15 .

1. INTRODUCTION

Rapid progress in development of high-current, medium-energy ion accelerators leaded to appearance of a new branch of neutron physics connected with desing, investigation and application of the intense neutron spallation sources. The principal idea of efficient neutron production is a conversion of ion kinetic

energy in heavy metal thick target to secondary particle radiation.

The spallation reaction of nuclei is the main mechanism for neutrons generation in passing of high-energy ions through matter. Besides neutrons, charged particles are generated to a large extent. However, as experimental studies and calculations have shown /1-4/, the relative share of neutrons quickly increases in the substance with propagation of the secondary radiation through it. Therefore even for comparatively small targets with the characteristic size above 100 g/cm^2 the neutrons yield by many times exceeds the charged particles yield. The most characteristic feature of neutron spectra of such sources is presence of the hard component in the energy range of hundreds MeV. This is more clearly illustrated in Fig.1, which shows the experimental spallation neutron spectra /2,5/ and a fission neutron spectrum for a comparison.

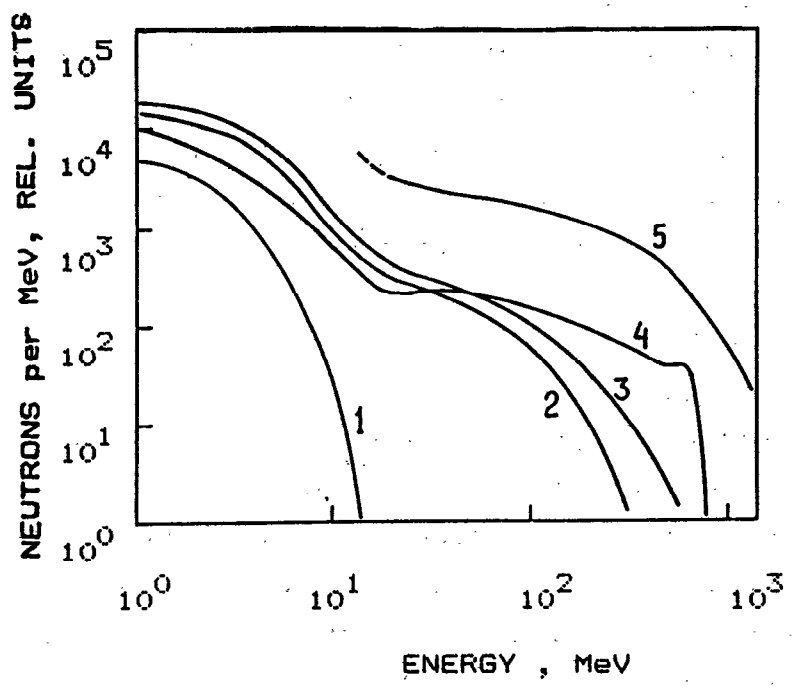

Fig.1 Energy dependence of the neutron production for fission source (1) and from medium-energy ion bombardment of various thick targets at emission angle Θ (the lines are eye-guide curves through the measured data points) : 2, 3 - 590-MeV and 1100-MeV protons on lead target 10 cm diam. x 60 cm long at Θ = 90° /2/; 4 - 800-MeV protons on tungsten target 3 cm diam. x 7.6 cm long at 30° /5/; 5 - 1-GeV/A ^{12}C ions on lead target 8x8x8 cm^3 at 30° / our results of TOF measurement /.

Meanwhile, in spite of high demand for studies of such neutron fields, there are no effective experimental methods enabling to carry out measurements under conditions of "bad" geometry. In the physics of low energy neutrons such studies are usually being done by the activation method or the method of fission threshold detectors. The latter method recently received its further development in work /6/ where the information taking from polymer solid state nuclear track detectors, SSNTD's, of fission fragments was automatized. This enabled to create an express method for determination of neutron fields' charts.

In this paper we briefly discribe the experimental method and its application to study the neutron field of thick lead target (20 cm diam. and 60 cm long) having a high neutron yield per incident ion. The considered energy region 1-3.7 GeV is the most interesting for the neutron sources design because it is characterized by a minimum of the ionization loss or a maximum of the neutron production per unit of ion kinetic energy. The precise measurements of the total yields of neutrons with energy less 15 MeV for this target were carried out by the neutron moderation technique by Vassil'kov et al. /7/. In present investigation the differential characteristics of the neutron source have been studied in detail.

2. EXPERIMENTAL METHOD

The most important requirement in construction of a hard neutron radiation detector is to broaden the existed standard set of fission threshold detectors by adding detectors with higher thresholds in the region of several hundreds or more MeV.

The detector chosen as one of such detectors was based on the bismuth's fission reaction that has been used in a number of works /8/ for registration of high energy neutrons. Study of the nuclear fragmentation of various materials, spallation reaction, under the action of high energy protons and neutrons allowed to construct a detector of new type with a very high value of the effective threshold above several hundreds MeV. For neutron measurements such a detector is used apparently for

the first time, and examining of its registering properties was paid special attention.

As to the design, a solid track detector of fission event presents a fissile layer about 1 mg/cm^2 thick, 11.3 mm in diameter (the area 1 cm^2) on an aluminum backing 19 mm in diameter and 0.2mm thick, placed close to the SSNTD. A spallation detector consists of two similar thick spallation layers (disks) embracing the track detector on both sides.

Such a design of the detector provides, firstly, a rather high efficiency of neutron registration due to making use of thick layers (the layer's thickness being greater than the maximum range of a fragment); secondly, sharp decrease of the detector's sensitivity dependence on its orientation relative to the direction of the neutrons' incidence by registration of fragments escaping both forward and backward; thirdly, shielding of SSNTD from other neighbouring material sources of background counting.

Fission and spallation products were registered by means of a SSNTD based on polyethylene terephtalate, PETP, 6 μm thick. The irradiated SSNTD are etched for 60 minutes at a temperature 60 ± 0.1 ^{o}C in a KOH solution (the density 1.252 g/cm^2 at 20^{o} C). The efficiency of neutron registration by a thin layer threshold detector may be found by the formula

$$E = n \sigma_f \eta \quad ,$$

where n is the number of nuclei of the fissile nuclide per cm ^{2}, σ_f - the fission cross section, η - fragment registration efficiency (η = 0.515 for isotropic escape of fragments).

Neutron fission cross sections are well known in the energy region bellow 20 MeV, and their values are part of different nuclear data libraries, for instance, ENDF/B-V. To obtain the values for higher energies of neutrons, measurements' results /5,9,10/ were used. The registration characteristics of spallation detectors were studied on a proton beam because of absence of a source of monochromatic neutrons of high energy. Besides, it was assumed that the spallation process weakly depends on the type of the incident nucleon and has

an equal possibility. In Fig.2 the measured energy dependences of efficiencies for investigated detectors are presented. From Fig.2 , it can be seen that the Cu-Cu and Cd-Cd detectors have considerably higher energy thresholds, and besides, the behavior of their efficiencies is expressed more sharply near the threshold. Note the Cd-Cd detector has a higher efficient threshold than the Cu-Cu detector.

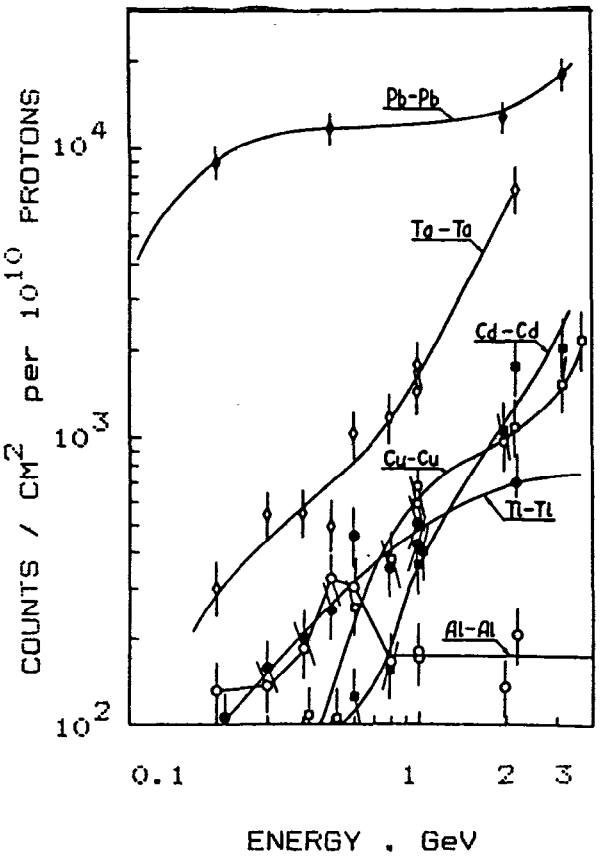

Fig.2 Energy dependence of nucleon registration efficiency for various thick layers measured on proton beam. The solid-lines are eye-guide curves through the experimental data points.

Thus, the following set of detectors were chosen, arranged in order to increase their registration treshold: U-235 in a cadmium or boron filter, Np-237, U-238, Th-232, Bi-209, Cu-Cu or Cd-Cd.

The energy dependences of efficiencies for a full set of threshold detectors, composing a neutron detector, are

presented in Fig.3. The detectors' response functions and the energy regions of maximum sensitivity for them were calculated on basis of these dependences . Analysis shows, that for all considered cases the detectors well complement one another and provide full coverage of a very broad energy range from thermal to several GeV.

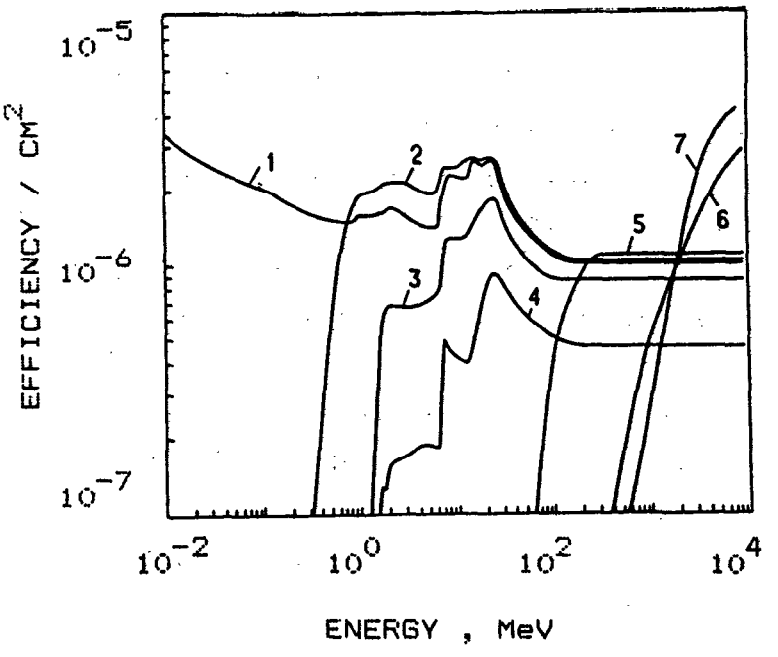

Fig.3 Energy dependence of threshold detectors' efficiencies for neutrons. The curves 1-5 are for fission detectors U-235, Np-237, U-238, Th-232 and Bi-209 respectively (1 mg/cm^2 thickness of fission layer). The curves 6,7 are for spallation detectors Cu-Cu and Cd-Cd.

For correction experimental data we studied the following distorting and background effects: 1) registration of charged hadrons; 2) angular assymmetry of fission fragments; 3) registration fragments from the backings ("the backing effect"), 4) spallation of nuclei of the fissile layer, 5) the own counting of SSNTD.

The registration characteristic and the reliability of the obtained results strongly depends on the method of processing of the irradiated SSNTD. In order to increase of the results' reliability, to decrease methodical errors, the thickness of the PETP film, was checked as well as the values characterising the process of SSNTD etching: the temperature, the concentration

of the KOH solution, the etching time.

Other sources of the errors are the uncertainties of the values of the layer's mass and the efficiency of registration of fragments, the errors of corrections for the background effects and the statistical error.

3. PROCEDURE OF DATA PROCESSING

The energy distributions of neutrons were reconstructed by iteration procedure using the results of integral measurements. The mathematical processing was realized in the computer code RESTOR. The results of data processing are the neutrons energy distribution, $F(T)$, and the yields of neutrons, $Y(T_i)$, with kinetic energy above T_i. The value T_i is choosed from the set (0 , 0.1 , 1 , 6 , 20 , 50 , 100 , 250 , 500 , 1000 MeV).

The program allows the operator to carry out visual control of the restoration process, detecting a disagreement between the experimental results of different threshold detectors. A small number of iterations (<10) is another criterion of agreement of data-in and a good choise of the zero approximation of energy distribution, $Fo(T)$. The zero approximation is realized in the code in two ways :

1) assignment of the table of values on the energy grid, using known results of measurements and the calculations of neutron spectra ;

2) analytic representation of the energy distribution.

The details of the measurement and data processing method take place in paper /11/.

The method was tested in the neutron field of a lead target (20 cm diam. and 20 cm long) irradiated by 2.55-GeV protons The three-component representation of neutron spectrum /12,13/ with realistic values of parameters was used for assignment of the zero approximation.

The results of measurements were compared with the ones obtained by the time-of-flight technique. The energy distributions measured by these experimental methods at angle 90° are presented in Fig.4. Good agreement of the results with each other in the

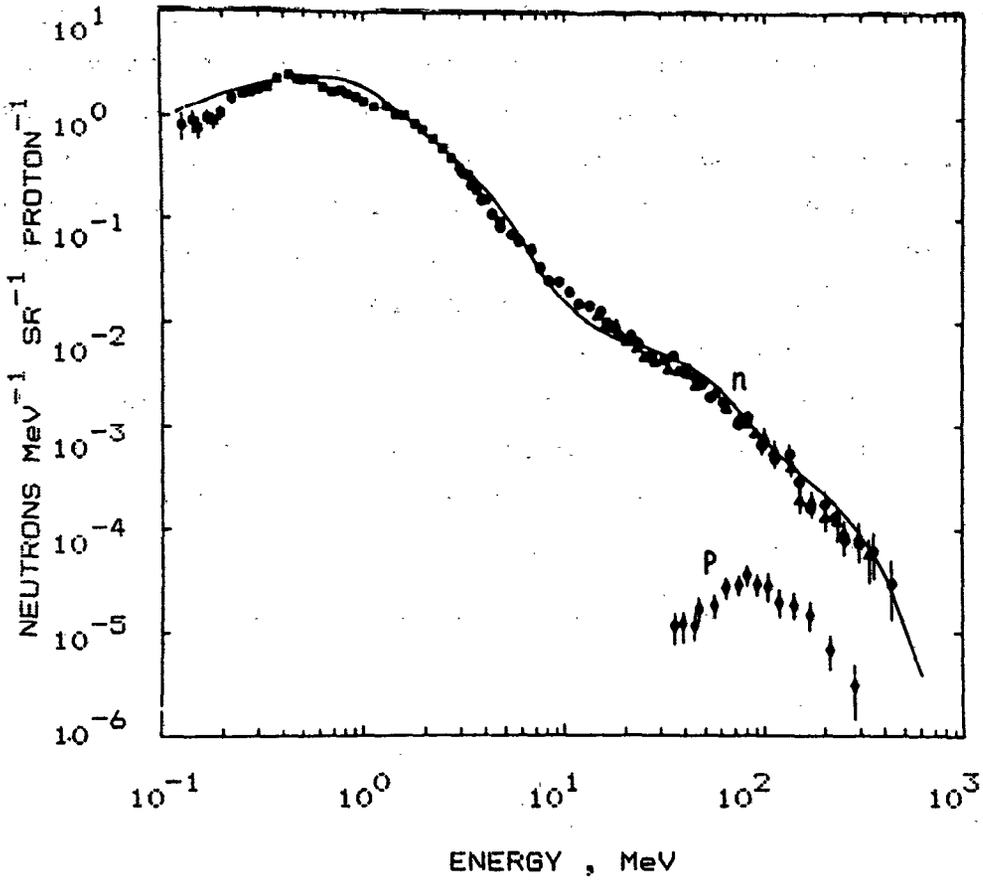

Fig.4 The spectral distribution of neutrons at emission angle 90° from bombardment of lead target 20 cm diam.x 20 cm long with 2.55-MeV protons has been measured by both the time-of-flight technique (the points) and the threshold detectors' method (the curve). The TOF spectrum of secondary protons is shown too.

whole energy range confirms applicability of the described method for studying the neutron fields of a hard energy spectrum.

As shown in Fig.4 , for thick lead target the neutron output is higher proton output more than order for all energies.

4. EXPERIMENTAL SETUP AND PROCEDURE

The neutron field of the lead target (20 cm diam. and 60 cm long) has been studied at synchrophasotron JINR using external proton and deuteron beams with energy about 1 , 1.5 , 2 , 2.5 , 3.1 , and 3.7 GeV. The beam intensity during the measurements

was typically of the order of a few 10^8–10^9 ions per second. The position and the profile of the beam at front surface of the target have been measured by multiwire proportional chamber. The beam spot at the target position as typically 20 – 30 mm (FWHM) in the vertical and horizontal directions. The ion flux has been monitored using activation reactions on aluminum $^{27}Al(p,x)^{24}Na$ and $^{27}Al(d,x)^{24}Na$. Aluminum monitoring-foil has been placed ~40 cm in front of the target. On a base of the experimental data for the first monitor reaction we have supposed the cross section about constant with a value 10.0±0.3 mb. But for the deuterons only in one experimental work /14/ a value of the cross section was determined 15.25±1.5 mb at energy 2.33 GeV. Our

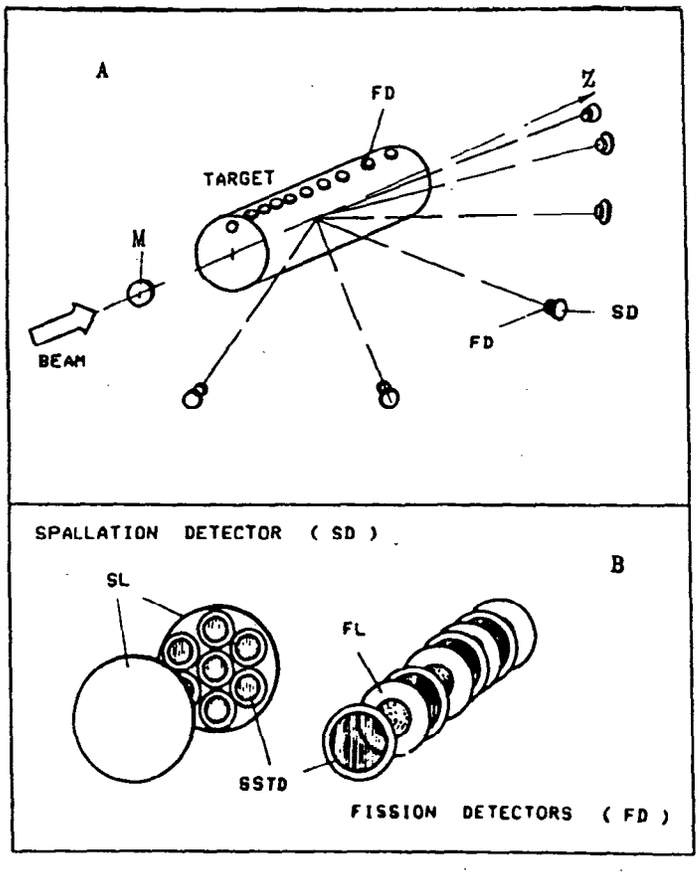

Fig.5 Schematic drawing of the target-detectors arrangement (A) and the construction of neutron detector (B) : M – aluminum monitoring foil ; FL – foil with fission layer ; SL – spallation layer.

relative measurements have shown that for the deuteron with energy 1-4 GeV a value of the cross section may be supposed about constant too. The experimental set-up and the neutron detector construction are shown in schematic Fig.5. The detectors have been placed along beam direction on the target surface and at angles of 10°, 30°, 60°, 90°, 120° and 150° at a distance 1 m from the centre of the target.

The typical neutron detector has consisted of the fission detectors and for angular measurements we have added the spallation detectors, where seven SSNTD's have been used for decrease of the methodical and statistical errors.

The measurements of the neutron background counts for different threshold detectors have been carried out with heavy concrete brick (50 cm long).

The data analysis has been performed by using our code RESTOR. The energy distributions mesured by time-of-flight technique for the lead target (20 cm diam. and 20 cm long) on 2.55-GeV proton beam have been used as a prior information to construct the zero approximation of the neutron spectrum.

The double differential neutron production distributions, $dF/dTdS$ and $dF/dTd\Omega$, have been determined for each value of beam energy. Then from these data the integral neutron spectra have been calculated for fixed values of the energy, $dY(T_i)/dS$ and $dY(T_i)/d\Omega$. Finaly, these differential distributions have been integrated for a determination of the total neutron energy spectra, $F(T)$ and $Y(T_i)$.

5. EXPERIMENTAL RESULTS

DIFFERENTIAL CHARACTERISTICS

The typical differential neutron distributions $dY(T_i)/dS$ on target surface along the direction of the incoming ions with energy 2.0 GeV is shown in Fig.6 All distributions have one maximum at Z = 12-22 cm. A value of the maximum position increases, when we pass from the total yield to the yield of the neutrons with energy T_i above 100 MeV, and besides with a rise of beam particle energy. An analysis of spatial dependent neutron production rates in the target shows that the most

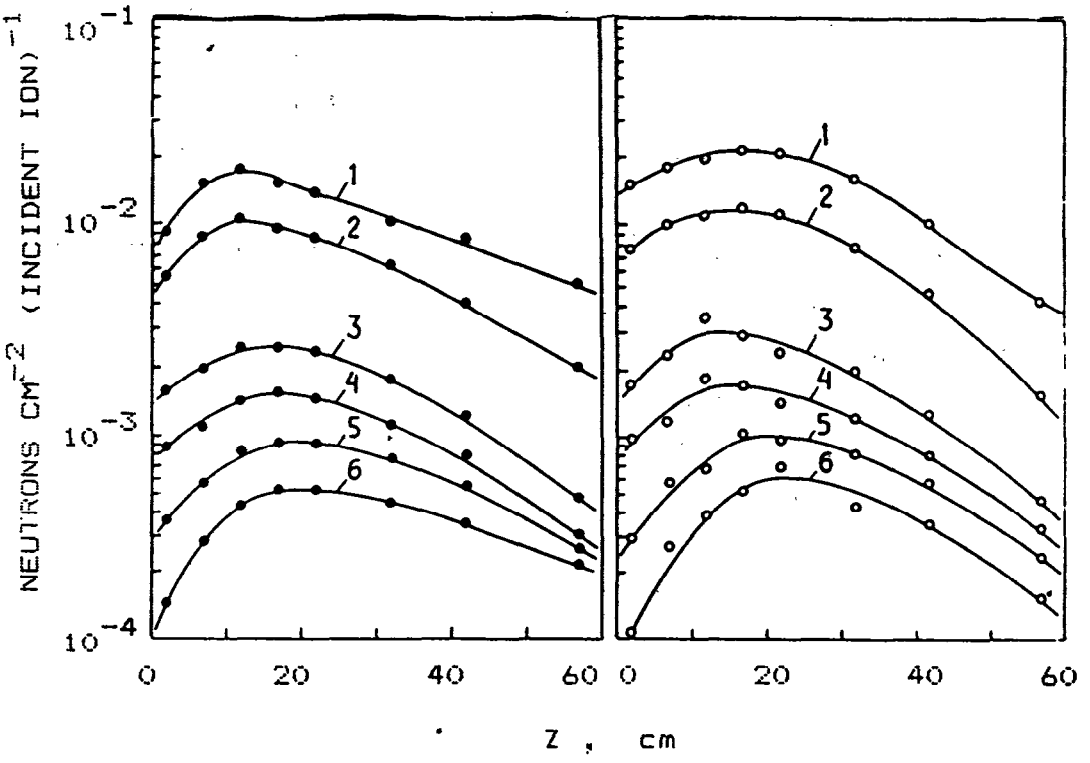

Fig.6 Side surface distributions of neutron production on the lead target by 2.0-GeV protons (●) and deuterons (O). The distributions 1-6 correspond to neutron energy above 0, 1, 6, 20, 50, 100 MeV respectively. The solid lines are eye-guide curves through the measured data points.

neutrons are emitted from the first half of the target (Z<30 cm). However the contribution of the second half of the target in the neutron yield increases to pass from 1-GeV to 3.7-GeV ions. The estimate has shown that about 87±4 % neutrons are emitted through the side surface of lead target and the contribution of the back surface in neutron emission only a few percents (this contribution increases as the beam energy rises). The angular dependences of the emission of neutrons with energy higher 1, 20 and 100 MeV, $dY(T_1)/d\Omega$, have been ploted in Fig.7 for the protons and the deuterons with energy 1 and 3.7 GeV. A comparison of a shape of angular distributions for the protons and the deuterons leads to a conclusion that only a few difference is observed between ones. The similarity of the shapes is partly place when the distributions measured at 1 GeV and 3.7 GeV are compared.

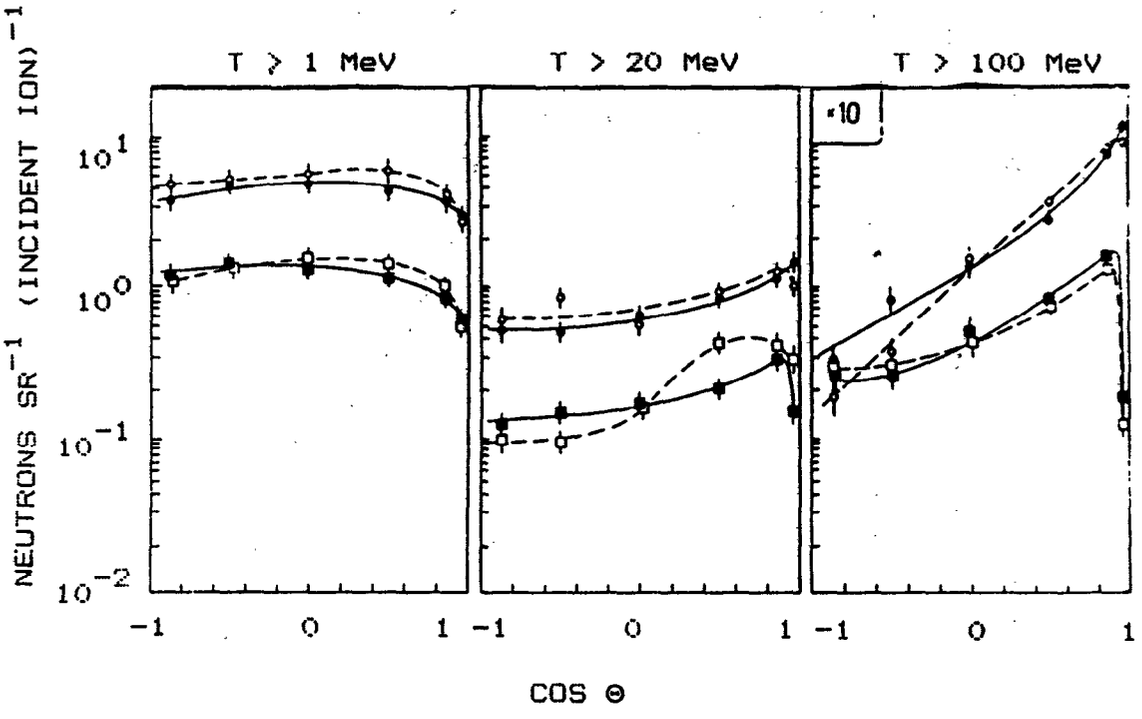

Fig.7 Angular dependence of neutron production with energy above 1 MeV , 20 MeV , and 100 MeV on the lead target by 1.0-GeV and 3.7-GeV protons (dark symbols and solid-lines) and deuterons (clear symbols and dotted-lines). The squares and circles correspond to 1-GeV and 3.7-GeV data. The lines are eye-guide curves through the measured data points.

In contrast, the shape of the distributions strongly changes moving to high-energy neutron region. The energy spectrum in the forward direction is much harder than in the backward direction and the angular distribution of the low-energy neutrons is more isotropic than for the high-energy component, which is strongly forward peaked.

INTEGRAL CHARACTERISTICS

The integral characteristics describe the production of neutrons for the whole target at all angles. As example, the absolute neutron energy spectra for incident protons and deuterons with energy 2 GeV are shown in Fig.8. This spectra have one maximum in the energy region 0.1-1 MeV and above a few MeV the intensity of both spectra monotonically and quickly falls with neutron energy. For protons the neutron spectrum is

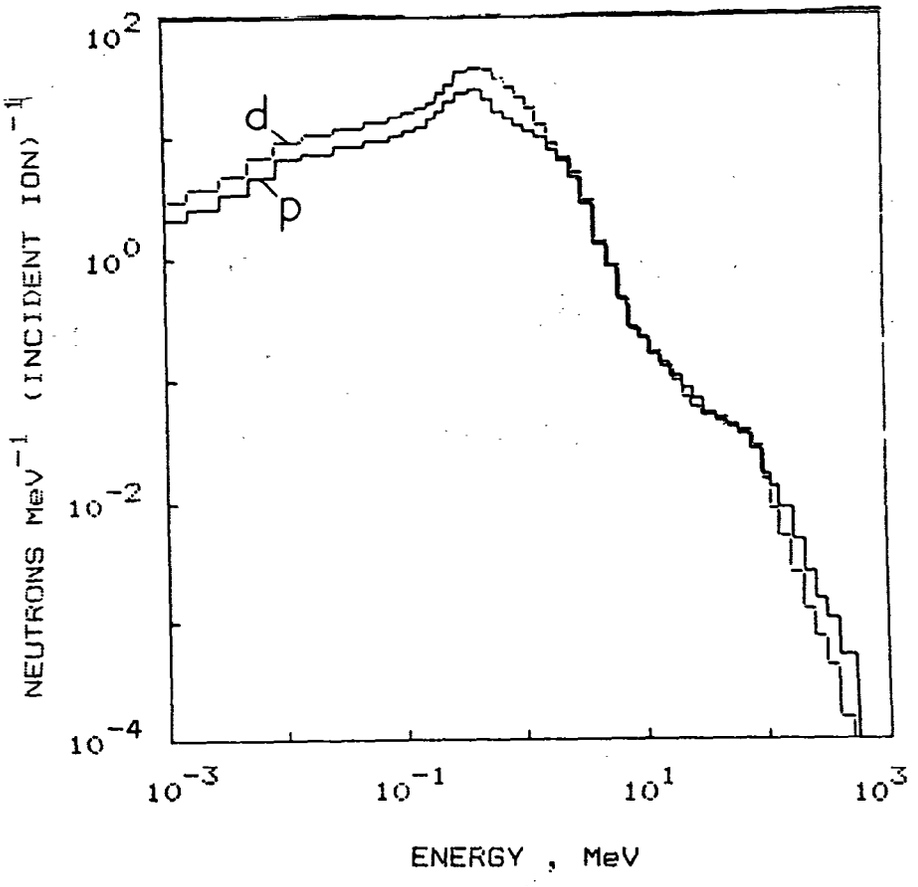

Fig.8 Comparison of the measured neutron energy spectra from the lead target bombarded by 2.0-GeV protons (solid-line histogram) and deuterons (dotted-line histogram).

more hard than one for deuteron which produce the most number of low energy neutrons but give the less high-energy neutron yield. The numerical values of secondary neutron yields at incident projectile energy about 1, 2 and 3.7 GeV are shown in Table 1.

Table 1. Experimental neutron yields for lead target (20 cm diam and 60 cm long).

energy group of neutrons	energy of incident ions /GeV/					
	protons			deuterons		
	0.994	2.00	3.65	1.032	1.98	3.76
total	25.1±3.0	44.2±3.1	80.7±6.9	24.9±5.0	58.5±8.2	98.9±14.
>1 MeV	16.3±2.1	27.5±2.0	49.9±4.5	13.9±2.8	31.3±4.7	56.6±8.5
>20 MeV	2.1±0.3	4.7±0.4	8.6±1.0	1.7±0.4	4.1±0.7	8.2±1.5

It should be noted that experimental error of data for deuteron beam is higher than one for proton beam. For deuterons, this leads to a large scatter of experimental points in the energy dependence of the neutron yield. As can be seen from Table 1, p and d ions produce in the lead target (20 cm diam. 60 cm long) about 38% and 45% neutrons in energy region below 1 MeV and about 10% and 7% above 20 MeV respectively. Our estimate of the

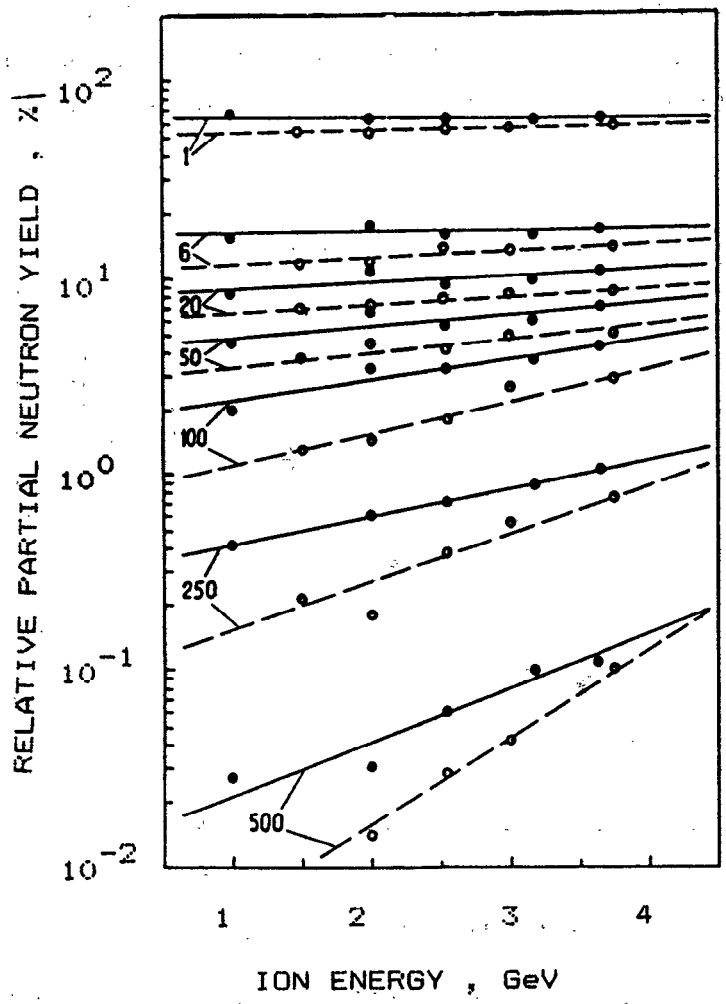

Fig.9 Relative partial neutron yields from the lead target as a function of incident ion energy for the neutron groups with energy above 1, 6, 20, 50, 100, 250 and 500 MeV. The data for the proton beam are the dark symbols and solid-lines, ones for deutron beam are the clear symbols and dotted lines. The lines are eye-guide curves through the measured data points.

average value of the total neutron yield ratio for various projectiles has given a result $Y_d/Y_p = 1.20 \pm 0.15$. The relative partial neutron yields as function of the incident ion energy have been plotted in Fig.9. As seen, their energy dependence becomes more strong for both types of the projectiles as the neutron energy is rising.

A comparison of the present experimental total neutron yields and the yields of neutrons below 15 MeV with the energy dependence of Vassil'kov et al. /7/ obtained by neutron moderation technique for proton beam and lead target (20 cm diam. and 60 cm long) is carried out in Fig.10. It shows a good

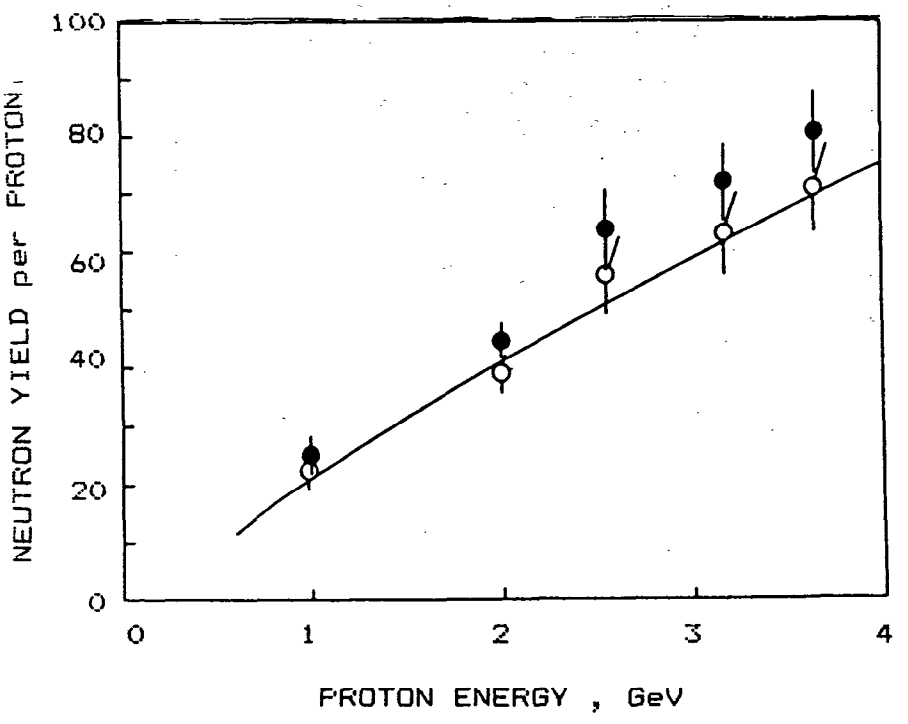

Fig.10 Comparison of the present results on total neutron yields (●) and the yields of neutrons below 15 MeV (O) with the energy dependence of Vassil'kov et al. /7/ obtained by the neutron moderation technique (solid-line) for the lead target (20 cm dium. x 60 cm long) bombarded by protons.

agreement between the present results for neutrons below 15 MeV and the dependence from paper /7/. A simple explanation of this is a neutron leakage. The neutrons with energies above about 15

MeV with high possibility go away from the moderator of experimental set-up.The data analysis is still being continued.

The authors would like to acknowledge the help in present measurements realization Y. M. Chirkin, N. S. Myzin, I. O. Tsvetkov, I. B. Vorob'ev.

REFERENCES

1. M. Nieminen, J. J. Torsti, Nucl. Instrum. Methods,v.179, 77 (1981).
2. H. M. Conrad, Nouvelle de SATURNE, n.8, 29 (1983).
3. A. R. Krylov et al., Report 16-85-347, JINR, Dubna (1985).
4. V. P. Bamblevsky et al., Report 16-86-486, JINR, Dubna (1986).
5. S. A. Wender et al., Proc. of the First Inter. Conf. on Neutron Physics, 1987, Kiev, Moscow, Atomizdt, v.4, 17 (1988).
6. I. B. Vorob'ev et al., Atomnaya Energiya, v.61, 35 (1986).
7. R. G. Vassil'kov et al., In this conference.
8. P. F. Denisov, V. N. Mehedov, Nuclear Reactions at High Energies, Moscow, Atomizdat (1972).
9. V. I. Gol'dansky et al., JETP, v.29, 778 (1955).
10. P. W. Lisowski et al., Proc. of the Inter. Conf. on Nuclear Data for Science and Technology, 1988, Mito, JAERI, 97 (1988).
11. I. B. Vorob'ev et al., Proc. of the 15th Inter. Conf. on Particle Tracks in Solids, 1990, Marburg, FRG (will be published in Nuclear Tracks in Radiation Methods).
12. T. Nakamura, Y. Uwamino, Phys. Rev. C, v.29, 1317 (1984).
13. T. Nakamura, Nucl. Instrum. Methods, v.A240, 207 (1985).
14. J. Banaigs et al., Nucl. Instrum. Methods, v.95, 307 (1971).